FDG PET Evaluation of Granular Cell Tumor of the Breast

Cornelia Hoess, Katja Freitag, Martin Kolben, Bernhard Allgayer, Irina Laemmer-Skarke, Walter B.J. Nathrath, Norbert Avril, Wolfgang Roemer, Markus Schwaiger and Henner Graeff

Department of Obstetrics and Gynecology, Institute of Radiology, Institute of Pathology and Department of Nuclear Medicine, Technical University of Munich, Munich, Germany

Granular cell tumor is a rare, usually benign neoplasm of neural origin that may arise in virtually any site and, when situated in the breast, can mimic breast carcinoma. We describe a case of granular cell tumor of the breast in a 57-yr-old woman. Clinical evaluation, mammography, sonography and MRI suggested a carcinoma with infiltration of skin and muscle. However, the tumor did not display increased glucose metabolism on PET. Clinical findings, imaging results, histological characteristics and surgical management are discussed.

Key Words: granular cell tumor; breast; PET; MRI

J Nucl Med 1998; 39:1398–1401

A granular cell tumor (GCT) is a rare neoplasm originating from perineural cells that have been described as occurring at almost any cutaneous or visceral site. When located in the breast (in 4.6%–16% of cases), the poorly circumscribed mass may mimic breast cancer despite its mostly benign nature (*1–4*). An accurate diagnosis is crucial because clinical evaluation, mammography, sonography and even frozen sections may suggest an invasive carcinoma and may lead to radical surgery.

Because (GCTs) occur most often in premenopausal women and rarely in men (*5*), they are thought to be estrogen dependent. Although Abrikossoff (*6*) first described GCT in 1926 as a myoblastoma, there is now sufficient ultrastructural and immunohistochemical evidence to support its origin from Schwann's cells of the peripheral nerve. Its characteristic histology and specific immunohistologic staining for S 100-protein and neuron-specific enolase have contributed to the current correct definition of GCT as a separate histological entity (*4,6–10*).

CASE REPORT

A healthy 57-yr-old nulliparous postmenopausal woman on estrogen substitution presented with a highly suspicious mass peripherally in the outer lower quadrant of the left breast with severe skin retraction. Axillary lymph nodes were slightly enlarged. Specific tumor markers CA15-3 and carcinoembryonic antigen were normal. Previous mammograms and ultrasonographic examinations (21 and 14 mo before admission, respectively) were reported as normal.

Mammography

Mammography performed at the time of admission revealed a 2 × 2 × 1.7 cm spiculated tumor in the mediolateral view associated with discrete microcalcifications in the outer lower quadrant of the breast close to the thoracic wall (Fig. 1). The mass was not seen in the craniocaudal view. A mammogram obtained 21 mo earlier was reported to be normal.

Ultrasonography

Ultrasound showed an irregularly defined solid mass with dorsal shadowing (Fig. 2). One enlarged lymph node and several nodes with regressive changes were observed in the axilla.

Magnetic Resonance Tomography

Magnetic resonance tomography was performed with a field strength of 1.5 T. Dynamic MRI of both breasts was performed after application of contrast medium (0.1 mmol/kg gadolinium diethylene triamine pentaacetic acid) as an intravenous bolus injection. Dynamic three-dimensional gradient-echo sequences (fast field echo; 15/5; flip angle, 40°) were acquired using a keyhole of 40%. Thirty-two transaxial slices with a slice thickness of 4 mm were obtained with a total of eight dynamic scans and a duration of 40 sec each. For image analysis, each slice of the dynamic dataset was evaluated for abnormal findings and increased signal intensity.

MRI showed a strongly enhancing lesion with pronounced rim enhancement in the outer lower quadrant (Fig. 3). The signal intensity increase in the first minute was more than 100% and was 140% in the second minute. A washout phenomenon was not seen.

PET

A PET scan was performed using a whole-body scanner consisting of 16 rings of bismuth germanate detectors yielding 31 transverse slices, at 3.4 mm apart. Emission data were reconstructed using iterative reconstruction after attenuation correction using transmission scans performed with ^{68}Ge rod sources. In accordance with our standard protocol (*11*), the patient fasted overnight before PET imaging to minimize blood insulin levels and glucose utilization in normal tissue. Standardized glucose metabolism also allows comparison of quantitative data of ^{18}F-fluorodeoxyglucose (FDG) uptake with other patients.

The study was performed with the patient in the prone position to avoid deformation of the breast. The emission scan of the breast was obtained 40–60 min after intravenous administration of 205 MBq ^{18}F-FDG. Attenuation-corrected images were reconstructed and normalized for injected dose and body weight, resulting in parametric images representing regional standardized uptake values (SUVs).

Visual analysis of radiographs revealed no evidence of focally enhanced tracer accumulation. Knowing the tumor location from other imaging modalities, such as mammography and magnetic resonance tomography, a small lesion displaying slightly increased tracer uptake could be evaluated (Fig. 4). Quantitative image analysis was performed using the average SUV in a region of interest drawn around the tumor using morphologic information from magnetic resonance tomography. The lesion displayed an average SUV of 1.8. In a population of 51 patients at our clinic, a threshold SUV of 2.5 was able to best differentiate benign from malignant lesions (*11*).

Received May 8, 1997; revision accepted Nov. 20, 1997.

For correspondence or reprints contact: Cornelia Hoess, MD, Department of Obstetrics and Gynecology, Klinikum rechts der Isar, Technical University of Munich, Ismaninger Strasse 22, 81675 Munich, Germany.

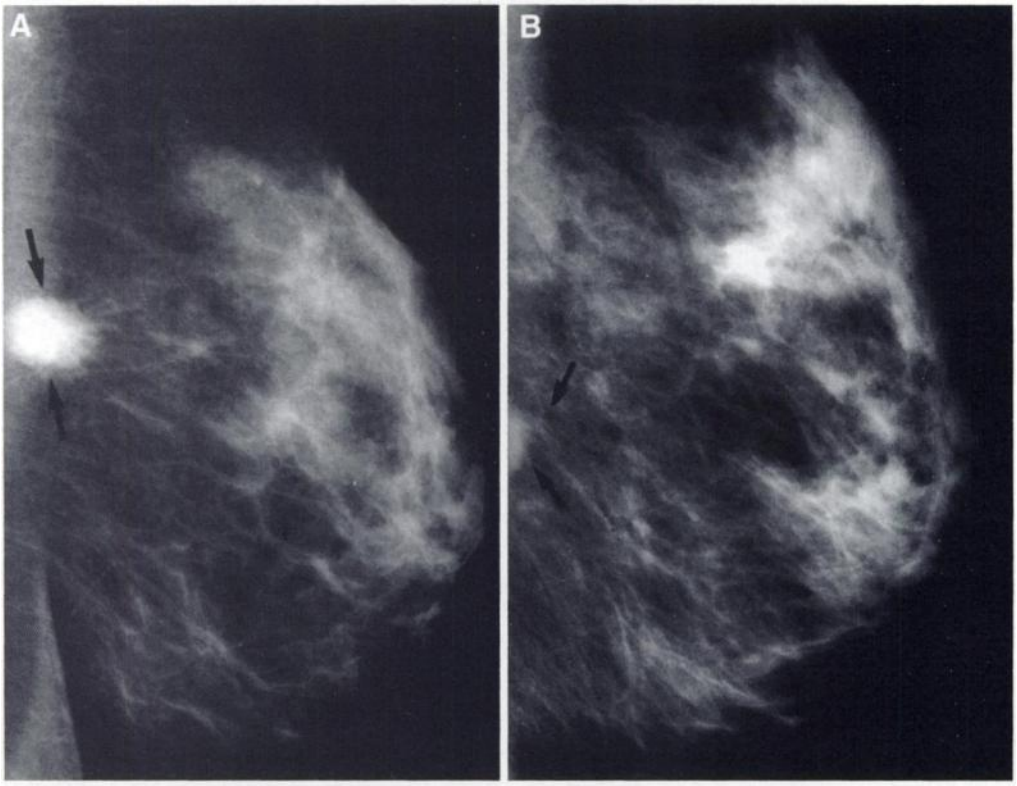

FIGURE 1. (A) Mediolateral mammogram of the left breast shows dense spiculated tumor close to the thoracic wall with some fine microcalcifications. (B) Mediolateral mammogram of the left breast 21 mo earlier. Retrospectively, the tumor is already visible in the left border of the film. The tumor was not depicted sufficiently because of incorrect patient positioning.

Surgery

A breast-conserving operation was planned with wide excision of the lesion including underlying fascia and superficial layers of the pectoralis muscle. After microscopic examination of frozen sections of the 2.2-cm tumor revealed an infiltrating growth pattern, an invasive ductal carcinoma was suggested and axillary node dissection was performed.

Histology

The final microscopic examination of the formalin-fixed and paraffin-embedded specimens identified the poorly circumscribed tumor with infiltration of subcutaneous and muscular tissue as a GCT with typical, abundant, granular eosinophilic cytoplasm and specific immunoreactivity for S-100 protein and without keratin antibody (Lu-5). No mitotic activity, MIB1 staining of less than 5% of the tumor cells and no immunostaining for progesterone or estrogen receptor was observed.

Using antibodies against factor VIII-associated antigen or CD 34, capillaries and small vessels were found to be concentrated in the outer zone of the tumor and within the fatty tissue bordering it. Interestingly, this staining distribution corresponded to the rim enhancement observed during MRI. Twenty-one axillary lymph nodes showed no metastases.

DISCUSSION

GCTs are rare. Their incidence is approximately 1 of 1000 tumors involving the breast (*5,12*). Most of them measure between 0.5 and 4 cm (*3,13,14*).

In contrast to their clinical appearance, which may strongly suggest a malignant lesion, most GCTs show benign behavior. Only a very few malignant cases have been reported (*13,15*).

Both our case and a review of the literature confirm that it may be impossible to correctly diagnose a GCT preoperatively using available imaging techniques. Since this tumor can mimic a solid malignancy in all morphological aspects (*16,17*), assessment of metabolism may be a more appropriate way to correctly diagnose this particular lesion.

Although several techniques are available for detecting breast cancer, only mammography is generally accepted as a screening method. Mammography is highly sensitive for detecting tumors but has a low specificity (10%–55%). Even in a postoperative reevaluation, mammographic findings were strongly suggestive of carcinoma in our case.

Contrast-enhanced MRI is gaining importance as an additional method for breast imaging, but its diagnostic value remains to be determined. The sensitivity of this method is reported to be higher than that of mammography, but specificity appears low. The appearance of early rim enhancement usually is interpreted as typical of a malignant growth pattern because of neovascularization within the outer zone and central tumor necrosis (*18*). In our case, a circular pattern of vascularization was found as well.

Recently, PET was introduced as a new method for evaluating breast masses. Few reports exist describing PET imaging of the breast (*19–21*). By using the radiolabeled glucose analog ^{18}F-FDG, this method allows for the visualization of increased glucose utilization in malignant tissue when compared with benign tissue. Initial results have been encouraging, because they report high sensitivity and specificity for detecting breast cancer. In our own experience of 84 patients with 111 histologically evaluated breast tumors, sensitivity ranged from 61% to 80% with corresponding specificity of 78%–98%, depending on image interpretation criteria (*11*). This new method is limited to detecting small masses, but for breast tumors larger than 1.0 cm high sensitivities and specificities (nearly 100%) have been shown. The main advantage of PET imaging seems to be its high positive predictive value in large masses and the ability to quantitatively assess FDG uptake in tumors. In this patient, quantification of FDG uptake using the SUV correctly

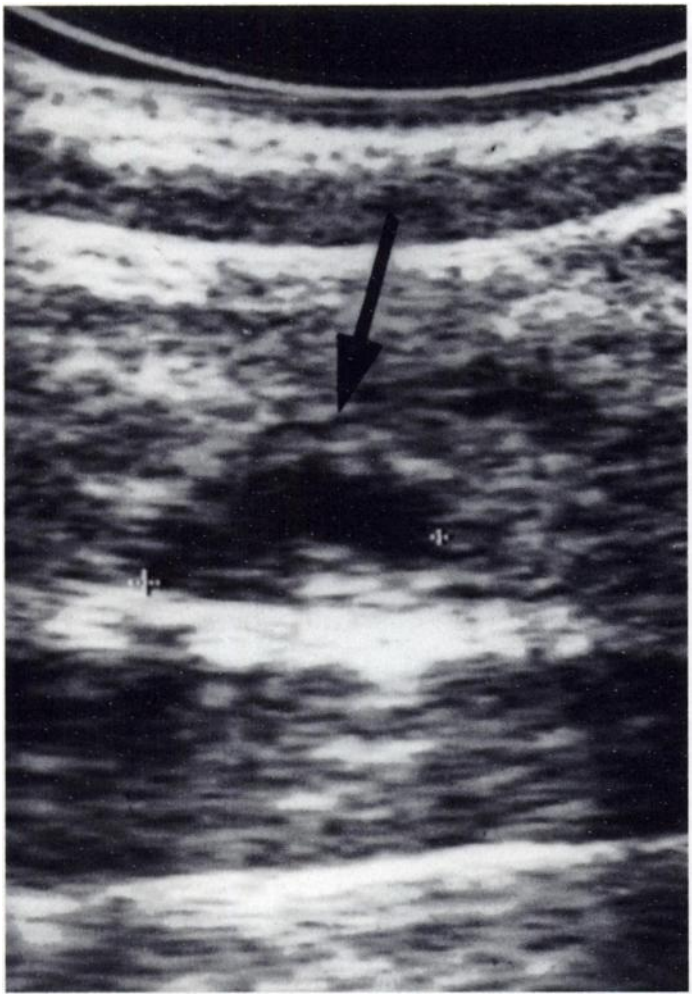

FIGURE 2. Ultrasonography of the left breast shows an ill-defined hypodensic solid lesion with enhanced through-transmission in the outer lower quadrant of the left breast.

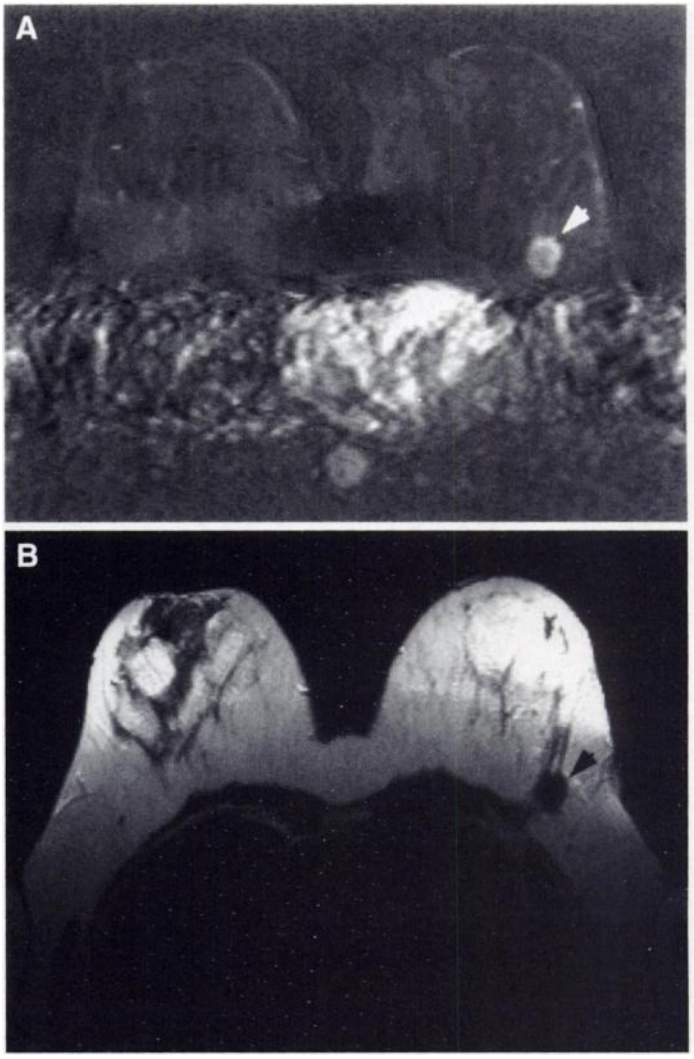

FIGURE 3. (A) T1-weighted postcontrast MRI in subtraction technique shows pronounced rim enhancement in the left breast, indicating malignancy. (B) T2-weighted MRI shows a hypointense spiculated lesion.

identified the lesion as benign. A previous study showed that an SUV threshold of 2.5 provides reliable differentiation between benign and malignant lesions. Thus, visual interpretation alone would not have led to a correct diagnosis (*11*).

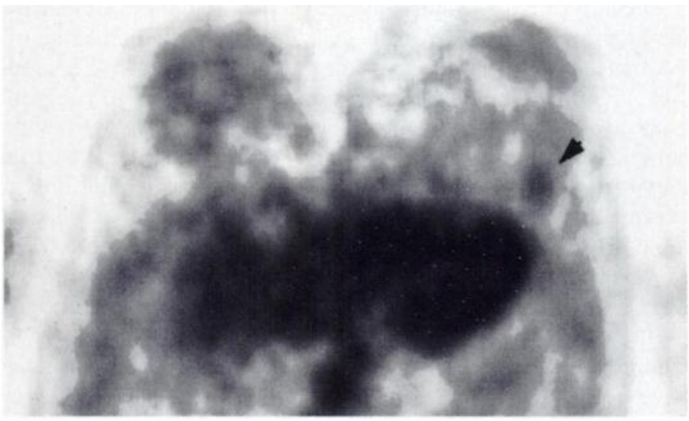

FIGURE 4. PET image shows enhanced fluorodeoxyglucose uptake in the left breast with a standardized uptake value of 1.8. Little activity is observed in the heart.

CONCLUSION

In contrast to clinical findings, mammography, ultrasonography, MRI and even microscopic frozen-section examination, FDG PET imaging can correctly differentiate GCT from a malignant tumor. Breast surgeons face the dilemma of accommodating the patient's understandable request for one-step surgery with the difficulty of establishing a definitive pre- and intraoperative diagnosis; therefore, they should be aware of the existence of GCTs (*21,22*).

REFERENCES

1. Bässler R. Pathologie der Brustdrüse. *Spezielle pathologische Anatomie*, vol. 11. Berlin: Springer; 1978:324–326.
2. van Doorn-Kaivers M, Billenkamp G. Granularzelltumor unter der Fehldiagnose szirrhöses Mamma-CA. *Geburtsh Frauenheilk* 1992;52:62–64.
3. Damiani S, Koerner FC, Dickersin GR, Cook MG, Eusebi V. Granular cell tumour of the breast. *Virchows Arch (Pathol Anat)* 1992;420:219–226.
4. Kalbfleish H, Louth G, Mühlberger G, Nitschke S. Das Granularcellmyoblastom der weiblichen Brust und seine differentialdiagnostische Abgrenzung gegen das Mammakarzinom. *Radiologe* 1978;18:143–147.
5. Mariscal A, Perea RJ, Castellá E, Rull M. Granular cell tumor of the breast in a male patient. *Am J Roentgenol* 1995;165:63–64.
6. Abrikossoff A. Über Myome, ausgehend von der quergestreiften willkürlichen Muskulatur. *Virchows Arch (Pathol Anat)* 1926;260:215–233.
7. Azzopardi JG. Histogenesis of the granular-cell "myoblastoma." *J Path Bact* 1956; 71:85–94.
8. Nathrath WBJ, Remberger K. Immunohistochemical study of granular cell tumours. Demonstration of neurone specific enolase, S-100 protein, laminin and alpha-1-antichymotrypsin. *Virchows Arch (Pathol Anat)* 1986;408:421–434.
9. Enzinger FM, Lattes R, Torloni H. Histological typing of soft tissue tumours. In:

Enzinger FM, Lattes R, Torloni H, eds. *International classification of tumours*, vol. 3. Geneva: World Health Organization; 1969.
10. Armin A, Connelly EM, Rowden G. An immunoperoxidase investigation of S-100 protein in granular cell myoblastomas: evidence for Schwann cell derivation. *Am J Clin Pathol* 1983;79:37–44.
11. Avril N, Dose J, Jänicke F, et al. Metabolic characterization of breast tumors with positron emission tomography using F-18 fluorodeoxyglucose. *J Clin Oncol* 1996;14: 1848–1857.
12. Gordon AB, Fisher C, Palmer B, Greening W. Granular cell tumour of the breast. *Eur J Surg Oncol* 1985;11:269–273.
13. Crawford ES, DeBakey ME. Granular cell myoblastoma. Two unusual cases. *Cancer* 1953;6:786–789.
14. Lellé RJ, Park H, Brow CA. Benign granular cell tumour mimicking carcinoma of the breast. *Eur J Gynaec Oncol* 1992;13:390–393.
15. Uzoaro I, Firfer B, Ray V, Hubbard-Shepard M, Rhee H. Malignant granular cell tumor. *Arch Pathol Lab Med* 1992;116:206–208.
16. Rickard MT, Sendel A, Burchett I. Case report: granular cell tumour of the breast. *Clin Radiol* 1992;45:347–348.
17. Kittner T, Dziambor U, Bergander S, Theissig F. Der Granularzelltumor der Mamma—die seltene Differentialdiagnose des Mammakarzinoms. *Röntgenpraxis* 1995;48: 185–186.
18. Heywang-Köbrunner SH, Beck R. *Contrast enhanced MRI of the breast*, 2nd ed. Berlin: Springer; 1995.
19. Adler LP, Crowe JP, Al-Kaisi NK, Sunshine JL. Evaluation of breast masses and axillary lymph nodes with (F-18) 2-deoxy-2-fluoro-D-glucose PET. *Radiology* 1993; 187:743–750.
20. Wahl RL, Cody RL, Hutchins GD, Mudgett EE. Primary and metastatic breast carcinoma. Initial clinical evaluation with PET with the radiolabeled glucose analogue 2-(F18)-fluoro-2-deoxy-D-glucose. *Radiology* 1991;179:765–770.
21. Hahn HJ, Iglesias J, Flenker H, Kreuzer G. Granular cell tumor in differential diagnosis of tumors of the breast. The role of fine needle aspiration cytology. *Path Res Pract* 1992;188:1091–1094.
22. Schneider V. Granular cell tumor in differential diagnosis of tumors of the breast. The role of fine needle aspiration cytology: letters to the case. *Path Res Pract* 1992;188: 1095–1097.

Intramedullary Fat Necrosis of Multiple Bones Associated with Pancreatitis

Byeong C. Ahn, Jaetae Lee, Kyung J. Suh, Kyung A. Chun, Sang K. Sohn, Kyubo Lee and Chun K. Kim
Departments of Nuclear Medicine and Diagnostic Radiology, Kyungpook National University School of Medicine, Taegu, Korea; and Division of Nuclear Medicine, Mount Sinai Medical Center, New York, New York

We describe findings of intramedullary fat necrosis on five imaging studies in a patient with alcoholic pancreatitis. Radiography and CT of extremities showed multiple osteolytic lesions that were initially considered to be metastases. However, a ^{99m}Tc-methylene diphosphonate whole-body bone scan revealed abnormal areas of increased uptake in only the bones of extremities without involvement of the axial skeleton, a distribution quite unusual for metastatic disease. Furthermore, ^{99m}Tc-sestamibi scintigraphy was essentially normal. MRI revealed findings compatible with the diagnosis of fat necrosis/infarct. Findings from bone biopsy demonstrated necrotic bone marrow without malignant cells. It may not be necessary to perform all the imaging studies described in this report when clinical features suggesting metastatic fat necrosis are present. Appearance and distribution of abnormalities on the whole-body bone scan and MR images show that necrosis/infarct of the marrow may obviate bone biopsy, which is often needed to confirm the diagnosis of intramedullary fat necrosis and to exclude neoplastic processes.

Key Words: pancreatitis; fat necrosis; radiography; scintigraphy

J Nucl Med 1998; 39:1401–1404

Pancreatic disorders can be complicated by fat necrosis at multiple distant sites, resulting in subcutaneous nodular lesions, polyarthritis and intramedullary fat necrosis (*1*). Although bone involvement of pancreatic disease had been believed to occur rarely, a necropsy study showed a relatively higher prevalence of bone lesion in postmortem samples with acute pancreatitis (*2*). The appearance of intramedullary fat necrosis on most imaging studies can be nonspecific, especially when an individual study is interpreted alone. We describe various radiologic and scintigraphic findings that led to the correct diagnosis in a patient with clinical features suggesting intramedullary fat necrosis.

Received Aug. 8, 1997; revision accepted Nov. 6, 1997.
For correspondence or reprints contact: Jaetae Lee, MD, Department of Nuclear Medicine, Kyungpook National University Hospital, Samduk 2 Ga-50, Taegu 700-412, Korea.

CASE REPORT

A 69-yr-old man with pulmonary emphysema was admitted for pain in the extremities that had worsened over several weeks. He had been experiencing upper abdominal discomfort concurrent with the appearance of extremity pain that partly subsided after fasting. His medical history included smoking for 35 yr and alcoholism with multiple previous episodes of alcoholic pancreatitis. Three years earlier, the patient was found to have mesenteric fat necrosis associated with pancreatitis during emergency exploratory laparotomy that was performed because of suspicion of acute intestinal infarction.

On admission, physical examination of the patient showed an emaciated body habitus and a soft, nontender, subcutaneous mass

FIGURE 1. A subcutaneous nodule is visible in the left deltoid area.